Terrestrial cosmic rays

by J. F. Ziegler

This paper reviews the basic physics of those cosmic rays which can affect terrestrial electronics. Cosmic rays at sea level consist mostly of neutrons, protons, pions, muons, electrons, and photons. The particles which cause significant soft fails in electronics are those particles with the strong interaction: neutrons, protons, and pions. At sea level, about 95% of these particles are neutrons. The quantitative flux of neutrons can be estimated to within 3×, and the relative variation in neutron flux with latitude, altitude, diurnal time, earth's sidereal position, and solar cycle is known with even higher accuracy. The possibility of two particles of a cascade interacting with a single circuit to cause two simultaneous errors is discussed. The terrestrial flux of nucleons can be attenuated by shielding, making a significant reduction in the electronic system soft-error rate. Estimates of such attenuation are made.

Introduction

This paper covers many fields, as diverse as elementary particle theory and computer system design. Its purpose is to connect cosmic ray physics to the field of electronic reliability. Definitions of well-known specialized words, such as hadrons or error-correction code, are provided in order to make the paper accessible to both engineers and scientists. We request the reader's tolerance of these definitions, with reliance on Mark Twain's aphorism: "One must never underestimate the pleasure one gives an audience by telling them something that they already know." The paper is organized as follows.

Cosmic rays in space

The term *cosmic ray* does not have a clear scientific definition. It has been used since the beginning of the twentieth century to indicate the unknown energetic particles that interfered with studies of radioactive materials. By 1913 it had been discovered that cosmic rays came from outer space. It is now customary to subdivide cosmic rays into the following categories:

- Primary cosmic rays: Galactic particles which enter the solar system and may hit the earth.
- Solar cosmic rays: Particles in the solar wind, originating in the sun. These are sometimes included in the term *primary cosmic rays.*

0018-8646/96/$5.00 © 1996 IBM

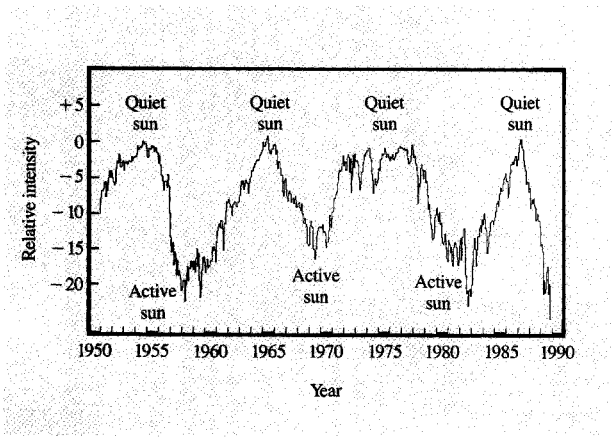

Figure 1

Cosmic ray flux at terrestrial altitudes. This plot is from the longest-running terrestrial cosmic ray monitor, which began operating in 1951 outside the Homestake Mine in Colorado. It shows the relative intensity (percent change from the 1954 flux) of the terrestrial cosmic ray flux with the solar cycle. Note that the solar cycle is raggedly sinusoidal, with each cycle being quite different from the others. Although these smoothed flux values show a variation of about 20% from solar peak to minimum, actual values may vary by >200% for daily averages, and much more for shorter periods. More than 99% of these particles originate from primary particles from outer space. The prime influence of the solar cycle is in its changes to the magnetosphere (which deflects incoming particles), and not in the production of terrestrial cosmic ray particles of solar origin. Data from J. A. Simpson, University of Chicago; private communication.

Table 1 Recent periods of the solar cycle.

Active sun	*Quiet sun*
1958	1963
1969	1974
1980	1985
1991	1996

- Secondary cosmic rays: Particles produced in the earth's atmosphere when primary cosmic rays hit atmospheric atoms and create a shower of secondary particles. These are also called cascade particles.
- Terrestrial cosmic rays: Particles which finally hit earth. Fewer than 1% are primary particles, and they are mostly third- to seventh-generation cascade particles.

The primary cosmic rays are believed to be produced and accelerated as a consequence of stellar flares, supernova explosions, pulsars, and the explosions of galactic nuclei. The cosmic rays in our galaxy have a mean lifetime of about 200 million years. Because our galaxy is spinning, there is a pervasive magnetic field of several micro-Gauss, and the cosmic rays interact with this field so that, typically, they spiral continually during their lifetime with a spiral diameter of a fraction of the galactic diameter. Because of this vast spiraling trajectory, a local observer can detect that the galactic cosmic rays are isotropic and do not come from particular sources.

The particles in space are 92% protons and 6% alpha-particles; the remainder are heavier atomic nuclei [1]. The galactic flux of primary cosmic rays is very large, about 100000/m^2-s. We shall see that the final nucleon flux at sea level is much lower than this, about 360/m^2-s, so few of the galactic particles have adequate energy to penetrate the earth's atmosphere.

A second source of primary cosmic rays is the sun, with its eleven-year cycle; see **Figure 1**. This plot is for a detector which has run for forty years in Colorado, and it gives a good picture of how terrestrial cosmic rays vary over time because of the solar cycle.

Solar particles have much lower energy than galactic particles. In general, particles need very high energy to create a cascade which can penetrate to sea level. The minimum energy required is generally accepted to be above 1 GeV, with the exception of a particle with a trajectory directly down into one of the earth's magnetic poles. During the period of quiet sun, e.g., 1985–1986 (see **Table 1**), there are effectively no particles in the solar wind which are energetic enough to penetrate to sea level on earth. During the active sun period, the number of solar particles hitting the outer atmosphere increases by a millionfold, and it is larger than the flux of intra-galactic cosmic rays. Some of these particles have energies which can reach terrestrial altitudes. During periods of a large solar flare, which might last a few days and often produce solar particles with abnormally high energies, the total intensity of cosmic rays at the earth's surface might double.

However, there is a secondary aspect to the solar cycle. The active sun with its large solar wind creates an additional magnetic field about the earth, and this field increases the shielding against intra-galactic cosmic rays. The effect is to reduce sea-level cosmic rays during the period of the active sun by about 30%. For complex reasons, the peak and minimum of this sea-level effect lag the solar cycle by about one or two years, so we can expect the next maximum of sea-level cosmic rays about the summer of 1998.

Satellite measurements of the primary cosmic ray particles are shown in **Figure 2**. If these particles start to penetrate the earth's atmosphere, they probably hit an atmospheric atom at an altitude above 50 km, starting a cascade of nuclear fragments.

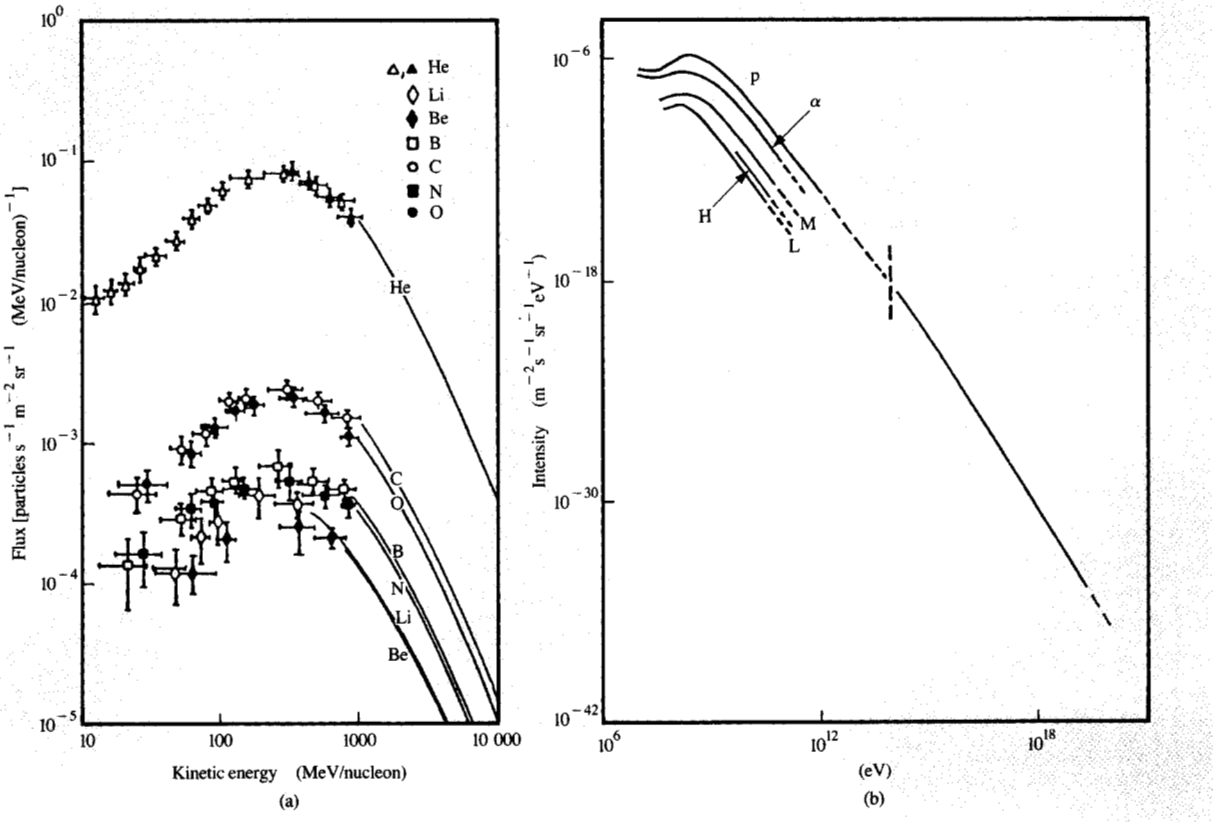

Figure 2

Flux of cosmic rays in space. The primary flux of particles incident on the outer atmosphere of the earth during a quiet sun period: Figure 2(a) on the left shows the lower-energy flux, with ions from He to O individually shown; Figure 2(b) on the right shows much higher energies; proton flux = p; He flux = α; light ions (Z = 3–5) = L; Z = 6–9 = M; and $Z > 9$ = H. Summed together, the primary flux averages 70% protons and 30% neutrons. From [2], reprinted with permission.

Cosmic ray cascades in the atmosphere

The study of cosmic ray cascades in the atmosphere has been reviewed extensively in many excellent books [3–11].

The earth's atmosphere consists of about 1033 g/cm^2 of oxygen and nitrogen, with a density which changes constantly with altitude. In cosmic ray physics, altitude is usually considered in units of g/cm^2 of the atmosphere above a given height. Sea level has an altitude of 1033 g/cm^2, and Denver has an altitude of 852 g/cm^2. These numbers are also the mean barometric pressure at these cities. Using the unit g/cm^2 for altitude removes much of the complexity of dealing with the physics of a material which has a constantly changing density.

The atmosphere is so thick that particles with the strong interaction, e.g., nucleons and pions (these particles are called *hadrons*), have many collisions before they reach sea level. Since the strong interaction is so powerful, virtually none of the original primaries reach the earth's surface. Instead, they create a cascade of secondaries which create further cascades until some later-generation particles may reach sea level. The cascade particles consist mainly of pions, muons, nucleons, electrons, and photons.

For terrestrial cascade analysis, these particles differ mainly in their type of interaction with other particles, their lifetime, and their mass (see **Table 2**).

Hadrons lose energy very rapidly to atmospheric nuclei, and their energy is dissipated into nuclear fragments. Those which also have an electric charge lose energy constantly to the atmospheric electrons. The heavier particles are least deflected, causing narrow dense cascades, and the light particles form a more diffuse halo about the heavier particles.

Table 2 Physical characteristics of cosmic ray particles.

	Interaction type			*Mass* (MeV)	*Mean lifetime*
	Electromagnetic	*Strong*	*Weak*		
Pions	Y	Y		≈134	26 ns
Muons	Y		Y	≈106	2 μs
Neutrons		Y		940	≈stable
Protons	Y	Y		938	stable
Electrons	Y			0.5	stable
Photons	Y				stable

• *Cosmic rays at airplane altitudes*

It was noted above that fewer than one in a hundred primary particles can create a cascade which can reach sea level. The cascades do not continue to increase in number as they penetrate the atmosphere, for there are also many absorption processes. Most of the particles either decay spontaneously (pions have a mean lifetime of nanoseconds, muons about a microsecond), or they lose energy and reach thermal energies before reaching earth, and these particles are lost from the cascade. The maximum cascade density of particles occurs at an altitude of nine miles (15 km), or just above airplane altitudes (this is called the Pfotzer point [12]). Below this, there is a net loss of total particles in the cascades (**Figure 3**).

The peak of the cosmic ray intensity occurs at about 10–25 km, which is also the altitude of many commercial airplane flights. The density of particles at this altitude is not as well known as for either the space environment, where the flux is simplified by the absence of cascades, or terrestrial environments, where long-term analysis experiments have been running for up to 50 years. For airplane altitudes, we have only the results of a few airplane or balloon flights of short duration.

Recently, experiments on cosmic ray effects at airplane altitudes have been published by IBM, Boeing, and others [14, 15]. We do not review this specialized field, other than to note that the fail rate of electronics at airplane altitudes is about one hundred times worse than at terrestrial altitudes, as was predicted in an IBM paper 15 years earlier [16].

• *Cosmic rays at terrestrial altitudes*

Energetic cosmic rays at sea level appear in cascades which hit in a splash of particles in less than a nanosecond. We discuss this lower region in detail, for it determines the flux of particles at terrestrial sites. The net loss of particles below the peak particle density (at airplane altitudes) can be simply expressed in a quantity called an *attenuation factor* or *particle mean free path* or *absorption length*, L, which combines creation and absorption processes into a single parameter which allows the calculation of the net change of particle flux with atmospheric pressure or altitude:

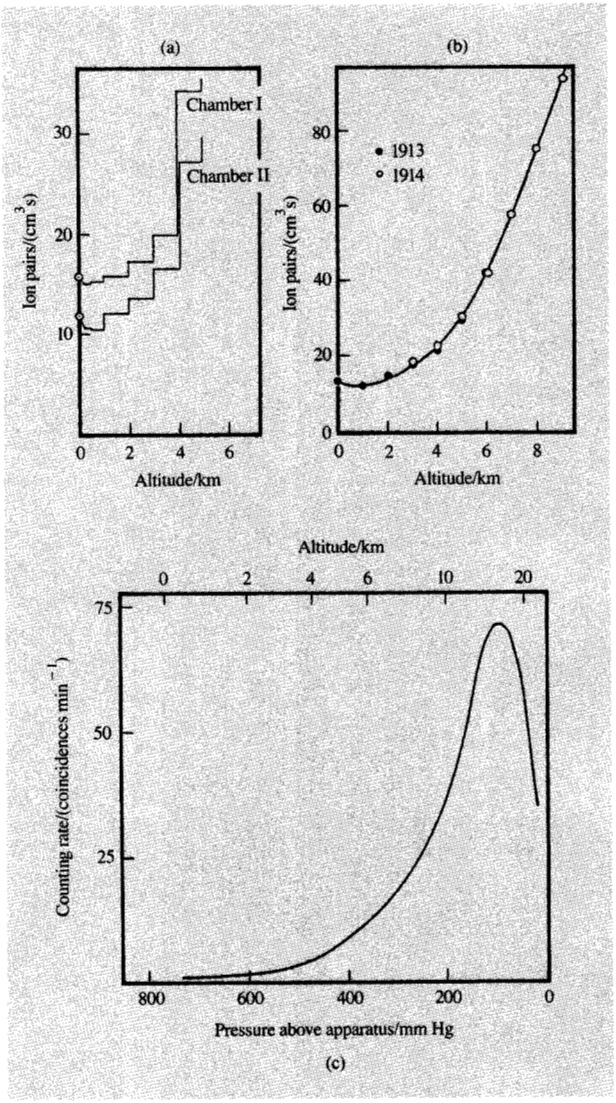

Figure 3

Earliest measurements of terrestrial cosmic rays. The measurement of the density of cosmic rays in the atmosphere won the Nobel Prize for Hess. In 1912 he used a balloon to take two ionization chambers up into the atmosphere to a height of 5 km, and showed that the flux of particles increased with altitude [see (a) and (b), the upper curves]. Although there were hundreds of measurements after this, it was not until 1936 that a detector was carried high enough to show that the cosmic ray flux peaked and then decreased at very high altitudes. The "Pfotzer curve," shown in (c), was named after the scientist who showed that there was an exponential increase in cosmic rays with altitude up to about 15 km, above which the cosmic rays decreased. The increase was a stunning 1000×, and for the first time it was realized how essential the thick atmosphere was to sustain stable life forms at sea level. From [12] and [13], reprinted with permission.

$$I_2 = I_1 \exp\left(\frac{A_1 - A_2}{L}\right), \quad (1)$$

where I_1 is the cascade flux at some altitude (pressure) A_1, and I_2 is the flux at altitude A_2, both altitudes being expressed in g/cm^2. To convert terrestrial altitudes to atmospheric pressure, g/cm^2, we use

$$A = 1033 - (0.03648H) + (4.26 \times 10^{-7}H^2), \quad (2)$$

where H is in feet and A is in g/cm^2 (this assumes an average barometric pressure and a temperature of 0°C). In the lower altitudes, typical absorption lengths are as follows:

Electrons: $L_e = 100$ g/cm^2,

Protons and pions: $L_p = 110$ g/cm^2,

Neutrons: $L_n = 148$ g/cm^2,

Muons: $L_\mu = 520$ g/cm^2. (3)

For example, if the neutron flux at sea level (height = 0 ft) is I, the neutron intensity at Denver (height = 5280 ft) is

$$I_{\text{Denver}} = I_{\text{sea level}} \exp[(A_{\text{sea level}} - A_{\text{Denver}})/L_n],$$

$$I_{\text{Denver}} = I_{\text{sea level}} \exp[(1033 - 862)/148],$$

$$I_{\text{Denver}} = 3.4I_{\text{sea level}}. \quad (4)$$

The absorption lengths between particles differ because of the strength of their interaction with the atmosphere, and their mass. A longer absorption length means slower attenuation, and hence less difference in flux when we compare locations with different altitudes. As an example of the magnitude of these factors, the increase in cosmic ray flux from New York City (1033 g/cm^2) to Denver (852 g/cm^2) is

Electrons: 611%,

Protons and pions: 518%,

Neutrons: 340%,

Muons: 142%. (5)

The one precaution to observe when using these numbers is that they do not describe the change of energy distribution with altitude, only the change in the total number of cosmic ray particles. (For experimental data on neutron attenuation factors, see the section on relative neutron flux.)

At sea level, there is a spectrum of particles which is typified by the flux at New York City (**Figure 4**). This is a theoretical calculation which is not as accurate as some experimental values to be shown later, but it shows the four most important particles and their relative abundance, normalized to the same site. Muons dominate the medium- and high-energy particle spectra. There are hundreds of

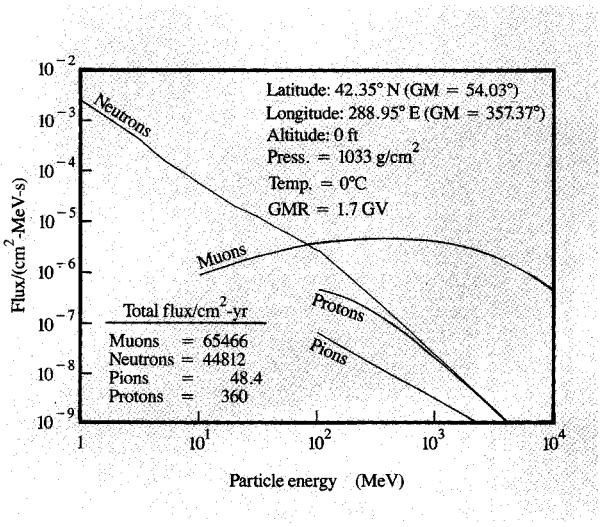

Figure 4

Theoretical sea-level cosmic rays. Theoretical calculation of the flux of cosmic ray particles at New York City. The most abundant particles are muons, which physically act like heavy electrons except that they are unstable and have a lifetime of less than 2 μs. The next most abundant particles are neutrons, which are very penetrating because they are neutral and do not lose energy to the electron sea of the atmosphere. There are just as many protons as neutrons produced in the upper-atmosphere cosmic ray showers, but the protons are charged and hence constantly lose energy to the atmospheric electrons and disappear faster than the neutrons at lower altitudes. At sea level there are fewer than 1 pion per 1000 muons, but we show that pions are far more effective in causing soft fails in electronic circuits. The above calculation is discussed later in the section on theoretical cosmic ray cascades [17].

times more muons than any other very high-energy particle. This is because the muons do not have the strong interaction and they lose energy only gradually to the atmospheric electrons. The same numbers of neutrons and protons exist at very high energies, but below 1000 MeV the absolute proton flux becomes less than the neutron flux because of the protons' additional electromagnetic interaction with the electrons of the atmosphere. The pion flux is small in relation to the other particles because their nanosecond lifetime causes most of them to fragment before they reach sea level. Finally, it should be noted that all sea-level particle fluxes below 100 MeV are very sensitive to local environments, i.e., the material of nearby walls, ceilings, and floors.

Note that in Figure 4 the latitude and longitude of New York City are converted to their equivalent geomagnetic (GM) values. The geomagnetic coordinates assume a sphere centered on the magnetic dipole of the earth, rather than on its spin axis. The North magnetic pole was located at 78.32 N and 68.95 W in 1980. Although the spin axis has a motion of about one meter per year down the 70 W

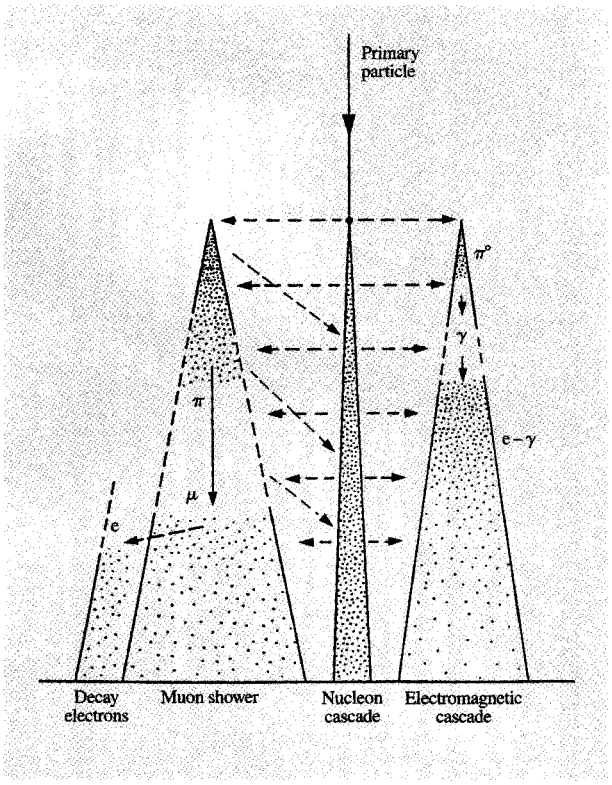

Figure 5

Schematic of cascades of various particles. The particle cascade from a very energetic primary particle can be described as a series of concentric cones. The innermost cone contains the heavy nucleonic particles of the cascade, and this is surrounded by cones which describe the relative spread of pions, then muons, and finally the light and easily scattered electrons. The figure shows these schematically, with the cones separated for clarity. Arrows also show where energy may be transferred from one cone to another as the cascade progresses.

meridian, the magnetic pole has very large motions based on (among other things) the solar cycle, the earth's orbital position, and lunar position. The magnetic field of the earth is found to vary the sea-level flux of cosmic rays by about 2×, and for this correction we must deal in geomagnetic coordinates.

Also noted for New York City in Figure 4 is the notation GMR, which stands for geomagnetic rigidity. This concept is discussed later, in the section on latitude effects on cosmic ray fluxes.

There are three important aspects of the cosmic ray cascades: the frequency of cascades, the spatial distribution of cascades, and the total flux of particles averaged over all cascades. The total number of particles allows us to estimate the number of soft fails which appear in a system over the period of a year. The spatial distribution of cascades allows us to calculate the probability that two soft fails occur in a system simultaneously and create a double fail in the system.

- *Extensive air showers*

At sea level, an "instantaneous" cascade may be as large as a million particles spread over a radius of a hundred meters and spread out in time to almost a nanosecond. The large cascades are usually called extensive air showers (EAS). An EAS may be defined as a shower detected on earth which has more than 10000 particles in it, or, equivalently, as a shower produced by a primary particle with an energy greater than 10^{14} eV. The EAS cosmic rays have been widely studied, and there is good agreement in their description [2].

We look at EAS events in some detail, since they allow us to estimate the probability of two soft fails occurring in a computer at the same instant (a condition which might cause mistakes to occur in computer memory error-correction codes).

The spatial distribution of a shower at sea level contains one or more *hot-spots*, the number of hot-spots being determined by the number of nucleons in the primary particle. For example, a He atom primary (He contains two protons and two neutrons) may create a cascade with four hot-spots, each of which may be a few meters apart from the others [6]. Each hot-spot can be further described as a series of concentric cones which intersect the earth—each cone indicates the distribution of a different type of cascade particle; see **Figure 5**. The narrowest cone is that of the neutrons, and the widest cone contains the easily scattered electrons and photons. At sea level, the spatial distribution of neutrons with energies between 200 and 3000 MeV (which is the energy of most concern for SER estimates) in the inner hard cone of an EAS may be described as follows:

$$\text{EAS neutron flux distribution: } F(r) = \frac{N}{r \exp\left(\frac{r}{60}\right)}, \qquad (6)$$

where N is the total number of particles in the shower and r is the lateral radial distance in meters (valid for $2 < r < 200$ m). The core area, $r < 2$ m, does not have a simple distribution because it depends on the details of the last collisions of the shower.

A typical EAS shower will spread uniformly over a hundred meters, since the cascade was initiated many kilometers up in the atmosphere. This means that over the area of a typical mainframe computer system (2m × 2m), the variation in nucleon particle density is small, and this area contains about 2% of the cascade particles. For a shower with 10^5 particles, experiments show that there is a central particle areal density of much less than 1/cm^2.

The EAS density is further reduced because the average shower comes in at about 45° (because of solid-angle considerations), creating an ellipse at the earth's surface. Only once in several years do sea-level detection arrays report central core particle densities which average above $1/cm^2$ [3].

The frequency of these EAS cascades falls off with size; see **Figure 6**, which shows summaries of various sea-level EAS experiments which have measured EAS frequency vs. shower particle number. Sea-level showers containing 10000 nucleons or more occur with a frequency of about $1500/m^2$-yr ($4/m^2$-day), and with 1000000 or more nucleons, about $2/m^2$-yr. This EAS frequency in units of (number/m^2-yr) goes as follows:

$$\text{Shower frequency} = 9 \times 10^8/(N^{1.4}) \quad \text{for } N < 10^6,$$
$$= 4.4 \times 10^{11}/(N^{1.9}) \quad \text{for } N > 10^6, \quad (7)$$

where N is the number of particles in the shower. These experimental expressions are for showers with $N > 10000$. For smaller showers the data are more erratic, but they follow the same trend; i.e., cascade frequency is inversely proportional to the size taken to about the power of 1.4. Integrating the cascade shower frequency over all sizes, we obtain for the total dose about $2.2 \times 10^9/m^2$-yr ($70/m^2$-s), about the same as the experimental $3 \times 10^9/m^2$-yr total nucleon dose of San Francisco [18]. If we look just at the EAS cascades, i.e., with $N > 10000$, the particles in these massive showers account for less than 1% of the total cosmic ray particles at sea level.

The data of Figure 6 may be combined in order to determine the probability of a simultaneous double soft fail in a memory array. We assume that the probability of a soft error of a bipolar cache memory chip has a cross section of about 4×10^{-12} cm^2/bit, with about 5×10^8 bits (64 MB) in the memory (see other papers in this issue for the range of chip sensitivity). The total number of energetic nucleons ($E > 20$ MeV) at sea level is about $10^5/cm^2$-yr ($13000/cm^2$-khr). Thus, the soft-error rate (SER) of the array is

Soft fails per year

$$= (\text{SER cross section})(\text{nucleon flux})(\text{number of bits})$$
$$= (4 \times 10^{-12}\ cm^2)(10^5/cm^2\text{-yr})(5 \times 10^8)$$
$$= 200/\text{yr}. \quad (8)$$

This rate indicates the need for error-correction codes (ECCs) for such large bipolar memory arrays.

A cache parity check occurs if the sum of the bits in a memory word does not agree with the parity bit. Each bit of a memory word is usually kept on a different chip from the others. Hence, a double error can occur in a single word only if two chips have a fail in the same word. To have a double hit on separate chips in a single cosmic ray shower, the cascade must be an EAS-type event. Since these contain only 1% of the nucleons, a double-hit probability is $<1\% \times 1\%$/(bits per chip), so to have a chance of a double hit within a year, the array SER must be in excess of 10^7 fails per year (assuming 1000 bits per chip). Hence, the need for double-correction ECC is not justified by cosmic SER rates.

Double hits can be caused by a single energetic nucleon hitting a circuit. This has been demonstrated for DRAMs which have been upset using a proton beam, and also for DRAMs at Denver [19]. High-energy proton testing of

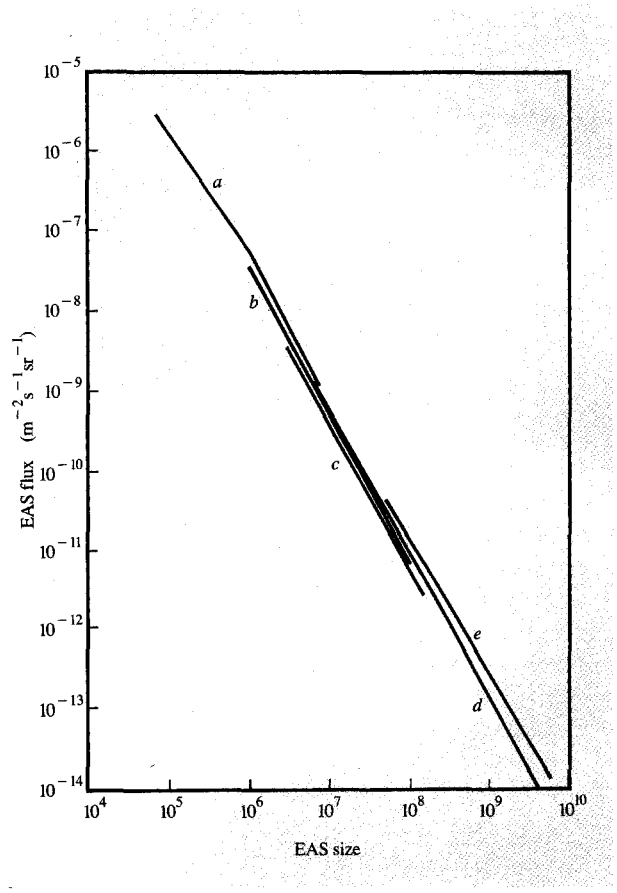

Figure 6

Cosmic showers: Frequency vs. size. The frequency of extensive air showers (EAS) at sea level is plotted as a function of the shower size. Each shower is the result of a single primary particle hitting the upper atmosphere. The data from various papers (labeled *a–e*) show the frequency of showers for cascades containing up to 10^{10} particles. The detector arrays are very large — some extend over a mile in diameter. The showers are very dilute; only rarely does the sea-level nucleon density reach $1/cm^2$. From [3], reprinted with permission.

bipolar SRAMs indicates that multiple fails from a single nucleon are rare [20].

Terrestrial cosmic ray spectra

This section is divided into separate sections for each of the major cosmic ray particles. Each section shows both experimental measurements and theoretical calculations. The calculation is shown not only for its fundamental aspects, but also to allow extrapolation of experimental measurements to other places. For example, it allows measurements taken in Japan, Italy, or India (three prime locations for sea-level measurements) to be converted to the equivalent flux at New York City. The theoretical formalism is summarized at the end of this paper.

- *Nucleon flux at sea level*

Most experiments which have measured the cosmic ray flux of particles with the nuclear force (hadrons) have not separated this flux into neutron, proton, and pion components. There is general agreement that the flux of particles is more than 97% neutrons at sea level, so the discussion below concerns primarily neutrons, with a special section devoted to the pion flux.

Neutron physics and electronic systems

This section uses simple physical arguments to show that most neutrons go through a circuit without an interaction (only one neutron in 40000 hits a silicon nucleus in the active top 10 μm of the circuit). But once a hit is made, there is a significant probability of a soft fail.

The neutron is a hadron particle with no charge and a mass of 10^{-27} g = 939 MeV = 1.0 amu. The strong interaction extends only about 10^{-13} cm from the particle, beyond which it disappears. It is this force which binds together the protons and neutrons which form the nuclei of atoms. Since the force is so limited in range, the cross section for interaction is estimated by the geometric cross sections of the nucleus (or one might say that the diameter of a nucleus is defined by the range of its strong interaction).

We can quickly estimate the probability of an energetic neutron interacting with a silicon circuit. Each nucleon (nucleon = either a proton or neutron) has a strong interaction radius of 1.3×10^{-13} cm. Silicon, which contains 28 nucleons, scales to a radius of about 4×10^{-13} cm. A nucleus of this size has a cross-sectional area of 5×10^{-25} cm^2. This circular area of the silicon nucleus is the cross section for interaction with neutrons. If the nuclei are uniformly distributed, they present a black wall (also called a total absorption cross section) to a neutron flux if their cross section can cover a plane; that is,

$$\text{Black wall} = [1/(\text{area/atom})] = (1/5 \times 10^{-25}\ \text{cm}^2) = 2 \times 10^{24}\ \text{atoms/cm}^2. \quad (9)$$

For silicon, with a density of 5×10^{22} atoms/cm^3, this thickness is

$$\text{Silicon absorption length} = (2 \times 10^{24}\ \text{atoms/cm}^2)/(5 \times 10^{22}\ \text{atoms/cm}^3) = 40\ \text{cm}. \quad (10)$$

We can now calculate the number of interactions that will occur near an LSI circuit on the surface of the silicon. Assuming that interactions must be within 10 μm of the surface to be important,

$$\text{Probability of nuclear ``hit''} = (\text{target depth})/(\text{absorption length}) = (10^{-3}\ \text{cm})/(40\ \text{cm}) = 1/40000. \quad (11)$$

One out of 40000 incident neutrons will interact within 10 μm of an LSI circuit.

As we discuss in detail later, at sea level there are about 10^5 neutrons/cm^2-yr with energies above 20 MeV. This means that every cm^2 of circuitry receives about $10^5/40000$ = 2.5 silicon–neutron hits per year in the circuit active volume.

We can now estimate how many of these neutron–silicon ``hits'' it takes to make a soft fail. The active device area on a typical chip may be about 0.04 cm^2, and if we assume that the devices have a 10-μm active depth typical of bipolars, the active volume of these chips contains

$$\text{Active atoms/chip} = (\text{active area})(\text{electrical depth})(\text{atom density}) = (0.04\ \text{cm}^2)(10^{-3}\ \text{cm})(5 \times 10^{22}\ \text{atoms/cm}^3) = 2 \times 10^{18}\ \text{atoms}. \quad (12)$$

Dividing the total active atoms of the chip's circuit by the absorption cross section of neutrons by silicon (estimated above) gives the cross section for a particle making a hit in the active volume of the circuit:

$$\text{Active cross section} = (\text{active atoms})/(\text{absorption cross section}) = (2 \times 10^{18}\ \text{atoms})/(2 \times 10^{24}\ \text{atoms/cm}^2) = 10^{-6}\ \text{cm}^2. \quad (13)$$

The accelerated testing paper in this issue [20] indicates that the soft-fail cross section for a 1986 bipolar memory chip is about 40×10^{-12} cm^2/bit (see Figure 13 of Reference [20]), and for a chip with 4096 bits, the chip SER cross section is 4096 bits $\times$ 40×10^{-12} cm^2/bit = 1.6×10^{-7} cm^2. The active absorption cross section is greater

than the SER cross section by $(10^{-6}\ cm^2)/(1.6 \times 10^{-7}\ cm^2) = 6$. One in six of the silicon–neutron "hits" results in a soft fail in these cache chips. If we reduce the active thickness of the circuit to about one micron, we can then estimate that almost *every silicon–neutron hit within one micron of an LSI circuit results in a soft fail.*

Altitude effects in the neutron flux

The relative density of the neutron flux at terrestrial locations may be estimated by using an exponential increase up to altitudes of 30000 feet; see **Figure 7** [21, 22]. This plot shows the flux of neutrons measured at various altitudes from sea level (1033 g/cm^2) up to space (0 g/cm^2). Taking a section across these curves at any energy produces a plot similar to the original Pfotzer data (Figure 3). One important point of Figure 7 is that there is remarkable similarity between sets of neutron spectra at low altitude [compare, for example, the curves for 1033 g/cm^2 (sea level) with those for 700 g/cm^2 (10 kft) and 400 g/cm^2 (23 kft)]. All of these curves are essentially parallel except for the highest-energy neutrons (which were inaccurate; see [23]).

From our discussion above, the net loss of neutrons with terrestrial altitude can be simply expressed in a quantity called an exponential attenuation factor, which combines the creation and absorption processes into the single attenuation parameter, A, shown in Equation (1). The attenuation length of the neutron flux has been measured by many authors; see **Table 3**. These numbers are in excellent agreement. We use 148 g/cm^2 as a value for the neutron attenuation length for terrestrial altitudes.

The accuracy of this number can be estimated by considering the possible differences of neutron fluxes going from New York City to Denver, Colorado. Going from New York City (altitude = 0 ft = 1033 g/cm^2) to Denver (5280 ft = 852 g/cm^2), the neutron flux increases by 3.4×.

This estimate can be compared to experimental measurements of cosmic ray SER as a function of altitude; see [21], Figure 6. Bipolar SRAM chips were measured at Leadville, Colorado, at Denver, Colorado, at sea level, and underground (under 5000 g/cm^2 of rock). The results are shown in **Table 4**. This table assumes that the sea-level flux is 94% neutrons, 4% pions, and 2% protons, and each scales according to the absorption rules stated above. Since the measurements were taken over a period of two years, the fail rates have been normalized to the mean cosmic ray sea-level flux intensity in 1990 using a cosmic ray monitor which accompanied the experiment to each site.

To estimate circuit SER at a site we need not just the neutron flux, but the total hadron flux (neutrons + protons

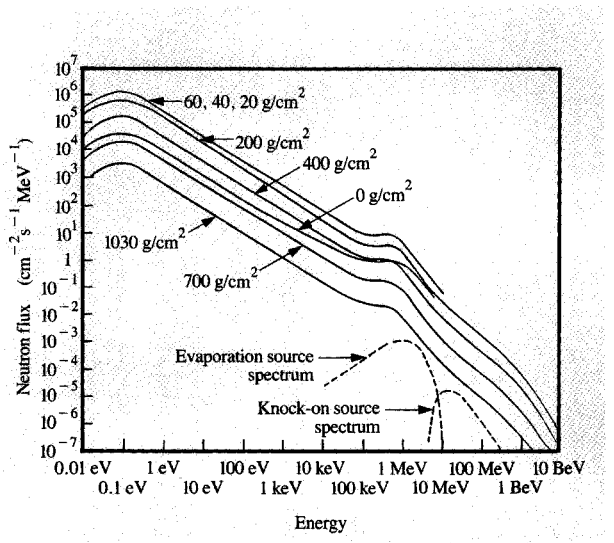

Figure 7

Neutron flux vs. altitude. The most comprehensive measurements of neutron fluxes in the atmosphere are called the "Hess values" [22]. This plot shows the flux of neutrons as a function of altitude up to outer space. The lowest curve, marked 1030 g/cm^2 (this is the thickness of the atmosphere), is for sea-level neutrons. The curve marked 700 g/cm^2 is for an altitude of about two miles. The neutron flux curves increase with altitude, and a cross section through them would result in a curve similar to the Pfotzer plot in Figure 3. The two dashed lines indicate the special nuclear reactions which cause the bumps in the flux curves from 1–100 MeV.

Table 3 Experimental neutron attenuation coefficients.

Neutron energy measured	*Neutron attenuation, L_n* (g/cm^2)	*Reference*
All energies	165	[24]
All energies	140	[25]
E_n: 1–10 MeV	143*	[18]
E_n: 10–100 MeV	150*	[22]
E_n: 50–1000 MeV	165	[26]
E_n: 10 MeV	144	[27]
E_n: 1–100 MeV	148	[28]
E_n: 80–300 MeV	150*	[29]

*Extensive study

Table 4 Experimental cosmic ray intensity vs. altitude.

Test site	*Altitude* (m)	*Barometric pressure* (g/cm^2)	*Theoretical change*	*Experimental change*
Leadville, CO	3100	692	12.7×	12.8×
Denver, CO	1610	846	3.9×	3.7×
Sea level	0	1033	—	—
Underground	−20 (rock)	−5000	≈0	No fails/ 10 mo.

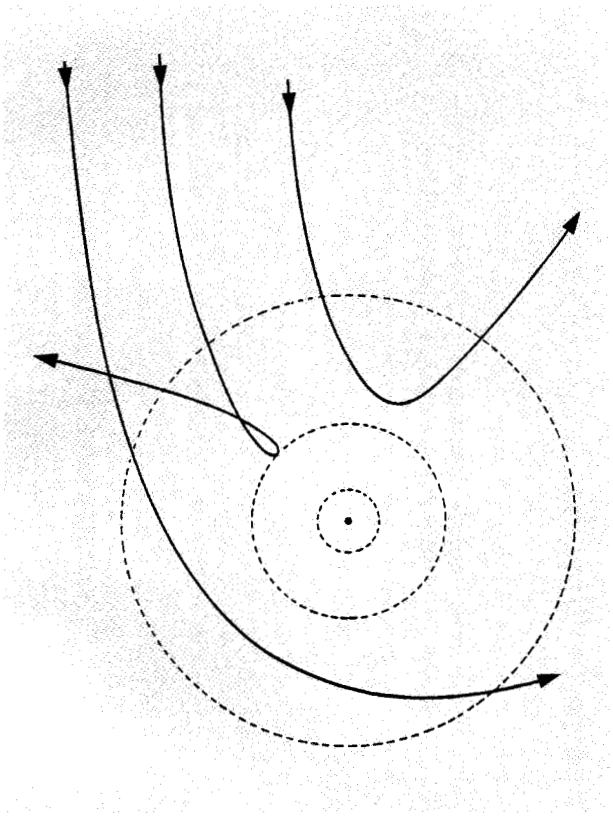

Figure 8

Trajectories of incident cosmic rays. The trajectories of incident cosmic rays are quite complex because of the earth's magnetic field. This diagram illustrates the possible paths which would be taken by particles with the same initial charge and momentum which are incident on the geomagnetic equator of the earth. The dashed circles indicate the magnetic shielding of the earth.

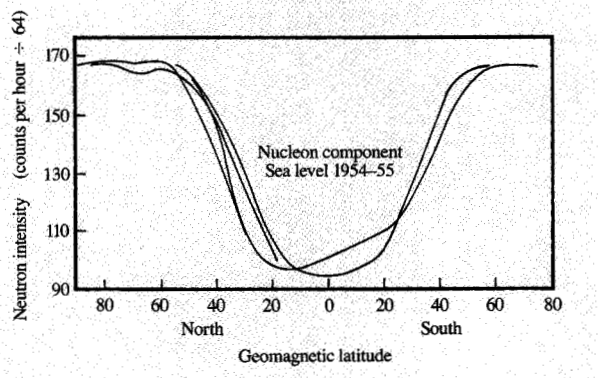

Figure 9

Cosmic ray intensity vs. latitude. In 1954–1955, a nucleon detector was transported at sea level back and forth from the Arctic to the Antarctic. The results, shown here, indicate that there is about a factor of 2 flux change from the geomagnetic equator to the pole. The nucleon detector was not well characterized, so it is unknown what energy of nucleons was being measured [31].

+ pions) at a location, since these particles at high energies have about the same nuclear cross sections [2]. We must add to the neutron flux ratio of 3.4 (calculated above) the contributions of other hadrons (protons and pions). The predicted nucleon flux ratio for Denver/sea level is shown in a later section to be about 3.9, in good agreement with the experimental value of 3.7.

Latitude effects in the neutron flux

The earth's magnetic field forms a shield against charged particles everywhere except for particles entering vertically into a pole. As primary cosmic ray particles near earth, the magnetic field interacts with the particle's charge and bends the particle's trajectory (**Figure 8**). If the particle hits an atmospheric atom and starts a cascade, each of the cascade charged particles will also have its path bent. This bending both increases the possibility that the particles will end up going back out into space, and lengthens the cascade path, reducing the probability that particles will reach sea level.

The effectiveness of the earth's magnetic shield in preventing sea-level cosmic showers is discussed in terms of the primary proton's "rigidity," which is defined as pc (p is the proton momentum and c is the speed of light). The units of rigidity are volts (V). Since the primary protons which can cause a sea-level shower are all highly relativistic, we can simplify this discussion by assuming their energy to be the same as their rigidity, but with the units changed from eV to V.

We define a terrestrial geomagnetic rigidity as the minimum energy that a primary proton must have to create a cascade which can reach sea level at a specific geomagnetic point.

Geomagnetic rigidities have been calculated for every location on earth (this work is constantly updated by the United States Department of Defense (US–DOD) because of the effect of cosmic rays on worldwide communications). Typical examples are shown in **Table 5**. This table shows that at a high geomagnetic latitude, e.g., Anchorage, Alaska, the rigidity is about 1 GV. Primary cosmic ray particles with energies above 1 GV may cause cosmic ray showers at Anchorage. This is the minimum energy to reach sea level, and it assumes that the particle has a vertical trajectory. If it is angled, it will take a much higher energy to cause a sea-level shower.

Near the geomagnetic equator, e.g., Tokyo, the geomagnetic rigidity is about 12 GV. Primary cosmic ray particles need energies above 12 GV to penetrate to

Table 5 Geomagnetic rigidity of various cities.

Geographic location	*Geographic Lat. Long.*	*Geomagnetic Lat. Long.*	*Altitude* (ft)	*Pressure* (g/cm^2)	*Rigidity* (GV)
U.S. east coast					
Boston, MA	42 N 289 E	54 N 357 E	0	1033	1.7
New York City, NY	41 N 286 E	52 N 353 E	0	1033	1.9
Washington, DC	39 N 283 E	51 N 350 E	0	1033	2.2
Miami, FL	26 N 280 E	37 N 347 E	0	1033	5.3
U.S. west coast					
Anchorage, AK	61 N 210 E	61 N 258 E	0	1033	0.98
Seattle, WA	48 N 238 E	54 N 294 E	0	1033	1.3
San Diego, CA	33 N 243 E	40 N 305 E	0	1033	6.0
Higher-altitude U.S. cities					
Chicago, IL	42 N 272 E	53 N 337 E	595	1011	2.1
Salt Lake City, UT	41 N 248 E	49 N 308 E	4390	881	3.1
Albuquerque, NM	35 N 253 E	44 N 316 E	4945	863	4.4
Denver, CO	40 N 256 E	49 N 317 E	5280	852	2.7
Leadville, CO	40 N 255 E	49 N 316 E	10200	710	2.7
Other cities					
Tokyo, Japan	36 N 140 E	25 N 206 E	0	1033	12.0
London, England	52 N 0 E	54 N 84 E	245	1024	3.1
Sydney, Australia	33 S 151 E	42 S 226 E	0	1033	4.9
Johannesburg, South Africa	26 S 28 E	27 S 91 E	5740	837	1.9

Tokyo. The geomagnetic rigidity can reach up to 17 GV right at the geomagnetic equator. There have been hundreds of experiments which have evaluated the concept of geomagnetic rigidities (in the early days, this was called the "latitude effect"). The measurement of the sea-level nucleonic flux is very complicated; we present the results in historical chronology in order to show the complex chain of experiments.

The earliest investigations of the latitude effect, from 1947 to 1953, were made in B-29 and B-36 bombers carrying particle detectors [30, 31]. Later detectors became too large for aircraft, and ships were used. **Figure 9** shows a set of shipboard nucleon flux measurements taken during 1954–1955 [32]. These experiments show the effects of geomagnetic latitude. It is clear from the data that the flux variation agrees better with the geomagnetic latitude than with the geographic latitude, which would be offset over 10° from that shown. A second feature of these data is that the flux variation occurs over a narrow band of 30°, with little variation within 20° of either the poles or the equator.

During the International Geophysical Years (1958–1967), a major effort was initiated by groups all over the world to quantify the cosmic ray nucleon flux and to determine its main parameters. Many groups constructed identical particle detectors which were cross-calibrated using a mobile standard detector. These detectors were sensitive only to nucleons with energies above 50 MeV, so their results are of particular importance to SER studies [23]. Typical results are those shown in **Figure 10**, for the nucleon attenuation length at widespread terrestrial locations. Some measurements were made at sea level and then at a different altitude by moving the detector. The difference in flux was then converted into an "attenuation coefficient" β, which is the inverse of the attenuation length we have used, and this coefficient was plotted in units of %/mm of Hg. In these units, an attenuation coefficient of 1.0 = 136 g/cm^2 absorption length. See the ordinate values on the right side of the plot to convert to g/cm^2.

Shown in Figure 10 are the results from 20 sites scattered around the world [34]. The results are very consistent, a tribute to the extensive research which went into the design of the identical detectors which were used, and to the fact that the groups were making relative rather than absolute measurements. The variation in mean attenuation length ranges from about 132 to 148 g/cm^2, and it shows a linear dependence on location rigidity. Data were collected from all latitudes from a special geomagnetic laboratory at the magnetic North Pole (Re) to two locations at the geomagnetic equator: Buenos Aires, Argentina, and Ahmedabad, India.

These IGY experiments measured both the proton and neutron fluxes together, so the neutron attenuation length (L = 148 g/cm^2) discussed before is mixed with a lower proton attenuation length (later measured to be about 110 g/cm^2). The proton value is lower than the neutron value, since it also loses energy by electromagnetic interactions, and thus protons are absorbed from the cascade faster. This combined nucleonic attenuation length is of great value for SER studies, since very high-energy protons and neutrons (>300 MeV) have identical nuclear reaction cross sections with silicon and we have to add their fluxes

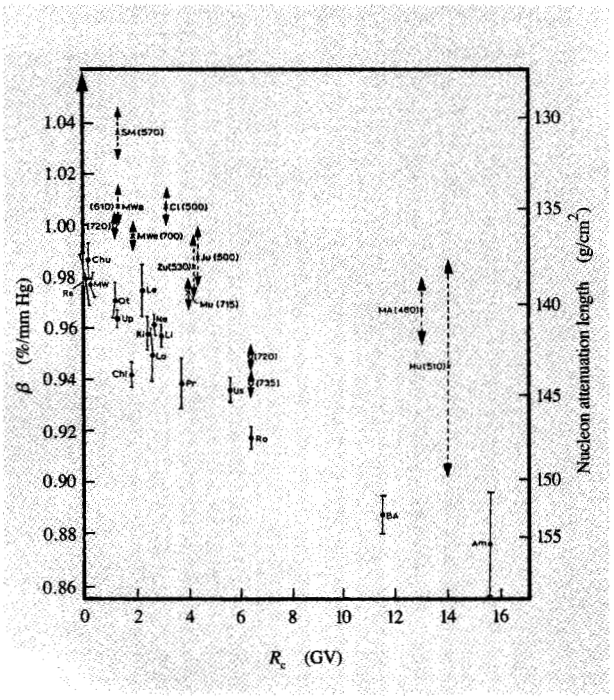

Figure 10

Terrestrial cosmic rays vs. geomagnetic rigidity. The nucleon attenuation coefficient β is plotted for 20 locations in an early attempt to measure comprehensively the cosmic ray flux on earth. The stations are plotted according to the geomagnetic rigidity of their location, which is a measure of the earth's magnetic shielding against cosmic rays. A rigidity of zero is shown for location Re (the Arctic weather station at the magnetic North Pole; Re stands for Resolute, for obvious reasons). At the far right are two locations at the earth's geomagnetic equator, Buenos Aires, Argentina (BA) and Ahmedabad, India (Am). The nucleon attenuation length is shown on the right ordinate: This is the inverse of the "coefficient" plotted as the left axis. The data show substantial agreement between groups with less than 10% separating values for the same rigidity. The identities of the various stations are cataloged in [33]. Reproduced from [33] with permission; copyright 1965 Società Italiana di Fisica.

dedication to the science of cosmic rays. Repeated measurements were made by many cosmic ray groups on the islands of Hawaii, ostensibly because they could park their detectors on Diamond Head and "let airplanes circle at the same altitude to cross-calibrate land and air-borne detectors while the balmy breezes cooled their Mai-Tai's" [36].

Typical results of these worldwide surveys are shown in **Figure 11**, where the inverse of the attenuation length is again plotted in units of %/mm of Hg—see the ordinate values on the right side of the plot to convert to an attenuation length in units of g/cm^2 [36, 37]. This figure shows the sophistication which was achieved near the end of the IGY years. The plot shows attenuation length vs. altitude and vs. geomagnetic rigidity, with both the calculations and the many data points coming together with remarkable consistency. At sea level (at a pressure of 760 mm Hg), the nucleonic attenuation length varies from 137 g/cm^2 for a geomagnetic rigidity of 1 GV, to 157 g/cm^2 for 13 GV. The attenuation length varies with rigidity because higher-energy primary particles create cascades with higher mean energies which have slightly lower interaction cross sections with the atmosphere and hence

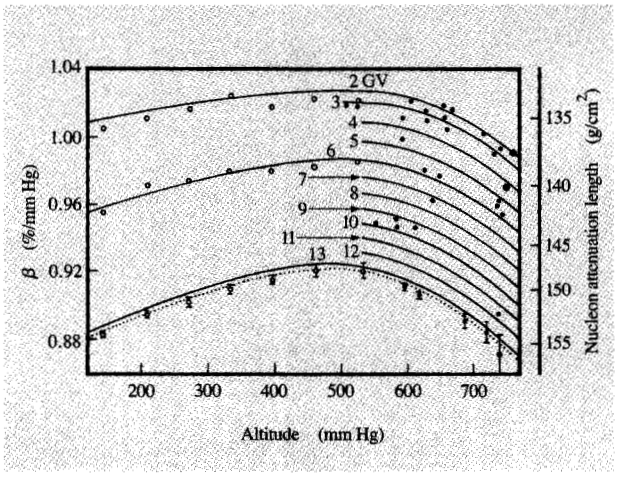

Figure 11

Cosmic ray intensity vs. altitude and rigidity. This figure is from the most comprehensive study ever made of the attenuation of cosmic rays on earth. Data from most of the locations described in Figure 10 are combined with data from mobile nucleon detectors on ships and airplanes to map out most of the earth. The detectors were sensitive only to nucleons with energies above 50 MeV, so these plots are especially useful for SER estimates. The nucleon attenuation coefficient β is shown to be a function both of altitude and geomagnetic rigidity. This is because both affect the energy distribution of the cascades, and the details of attenuation are energy-dependent. This beautiful study is like the last apple of the season: It is rich with flavor and detail, but it also contains a worm (see Figure 12) [37].

together. However, detailed modeling for the lower-energy range of 20–200 MeV may show significant proton/neutron differences, in which case the separate attenuation lengths for neutrons and protons are needed. Also shown is a smaller dependency on site barometric pressure, which is analyzed later.

The consistency of reported results like that in Figure 10 gave scientists confidence that measurements of cosmic rays could be conducted with accuracy and reliability, so in 1965 an international consortium (IQSY) began the complete mapping of the cosmic rays on earth [35]. Ships and airplanes were chartered for hundreds of cruises/flights with detectors going from the North Pole to the South Pole, with lengthy stays in most major cities in selfless

longer mean free paths. As discussed earlier, the difference between attenuation lengths of 137 g/cm^2 and 157 g/cm^2 would make the relative flux of cosmic rays at Denver vs. New York City vary by only ±10% from the mean, so this difference is only marginally important for SER work.

Also shown in Figure 11 is the effect of altitude on the mean free path of nucleons. As altitude increases (lower pressure on the abscissa), the attenuation lengths for all rigidities decrease up to an altitude of 11000 feet (500 mm Hg). This decrease has been attributed to the fact that the high-energy proton/neutron ratio in the cascades increases with altitude (at sea level the neutron/proton ratio is 5×, while at Denver it is about 3×), and the protons have a much lower mean free path than the neutrons because of their electronic energy loss. This lowers the total nucleon attenuation length.

Above 11000 feet there is an increase in the attenuation length because the mean energy of the cascades is increasing with altitude, and this increases the mean free path of the cascade nucleons. Cascades with higher energy are more penetrating.

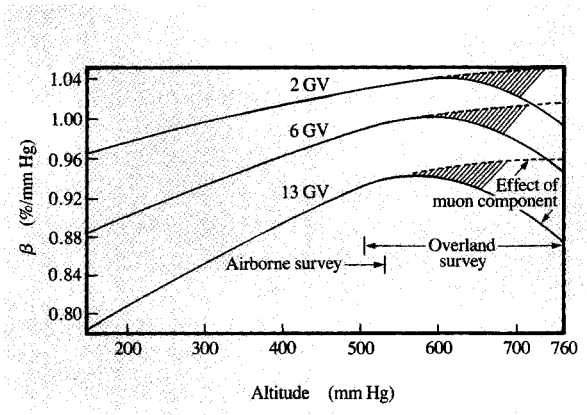

Figure 12

Mean attenuation coefficient for neutrons. An analysis of the results shown in Figure 11 showed that the proposed attenuation curves (solid lines in Figure 11) could predict the differences in nucleon flux recorded by the IGY detectors. However, the detectors did not accurately discriminate against other particles which were not nucleons. The most important example was an event called muon capture (described in detail in the section on muons), which generated neutrons within the detector. This figure shows how the attenuation coefficients must be altered so that they can be used to correctly predict the change of nucleon flux with altitude and geomagnetic rigidity. The muon capture effect disappears with altitude because its magnitude remains fairly constant with altitude, while the neutron flux continues to increase, finally making the muon capture error negligible. With this correction, the mean attenuation lengths should be accurate to about 1% [23, 36, 37]. From [23], reproduced with permission.

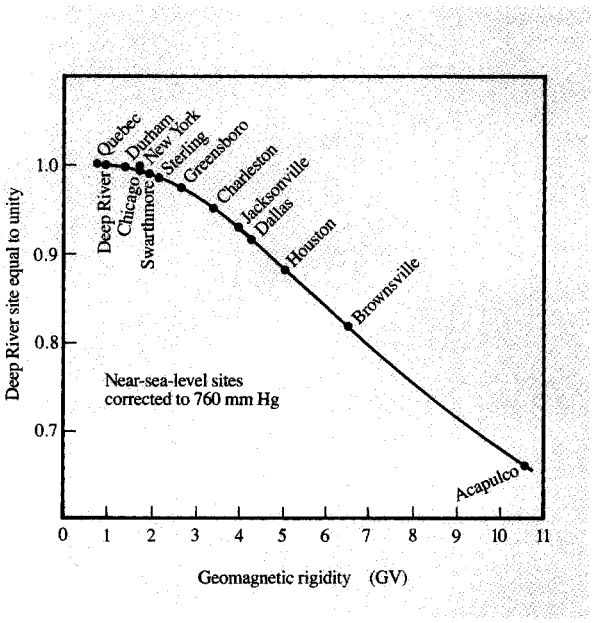

Figure 13

Altitude vs. geomagnetic rigidity. The preceding figures show how to scale the cosmic ray flux with altitude. This figure corroborates the variation of flux at sea level with geomagnetic rigidity. The data were produced by hauling a 23 000-lb detector to the various locations shown. The detector used was very sophisticated and reliable, and was sensitive only to nucleons with energies above 50 MeV. The resulting curve shows a reliable estimate of cosmic ray nucleon flux with geomagnetic rigidity. From [38], reproduced with permission.

The increased penetration of higher-energy cascades is also seen in Figure 11 in the change of attenuation length with geomagnetic rigidity. At sea level, the value of L is about 137 g/cm^2 for $GV = 2$, and it is about 156 g/cm^2 for $GV = 13$. The cascades at a 13-GV location will have a higher mean energy at sea level than those at a 2-GV location, and the higher mean cascade energy means a higher attenuation length, i.e., less attenuation [38].

A final matter makes the all-purpose attenuation lengths of Figure 11 a little less attractive than they originally seem. These attenuation lengths describe the IGY nucleon detector response, but they do not remove instrumental error, which was just being discovered when IGY was ending. One major factor was not included: the generation of neutrons by muon capture. This reaction occurs when a negative muon combines with a proton and produces one or more neutrons inside the detector (see the later discussion on the muon sea-level flux). About 7% of the measured sea-level neutrons in Figure 11 were from this source, causing a significant error.

The correction to Figure 11 is shown in **Figure 12.** The net effect of including the corrections is to decrease the

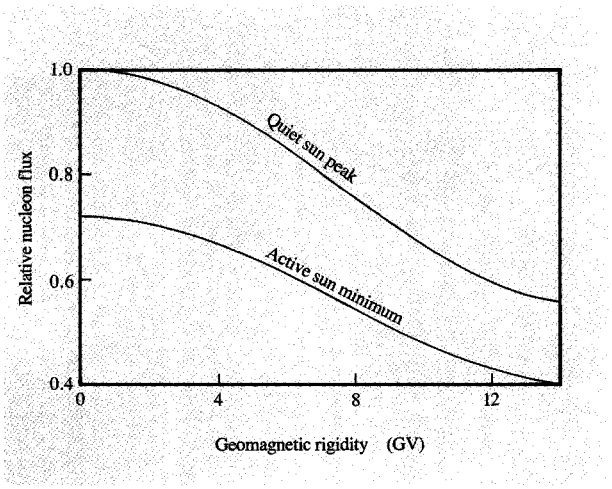

Figure 14

Cosmic rays vs. solar cycle. This curve results from an analysis of the sea-level portion of experiments like those shown in Figures 11–13 in order to determine how the results depend on the solar cycle. This can be considered the final tuning of our knowledge of the sea-level flux with geomagnetic rigidity [38].

Table 6 Variation of cosmic ray flux at various cities.

Geographical location	*Nucleon flux difference from NYC (%)*
Sea-level cities	
New York City, NY	0
Boston, MA	1
Washington, DC	−1
Miami, FL	−10
Anchorage, AK	2
Seattle, WA	1
San Diego, CA	−14
Higher-altitude cities	
Chicago, IL	16
Salt Lake City, UT	304
Albuquerque, NM	335
Denver, CO	388
Leadville, CO	1100
Arapahoe, CO	1700
Other cities	
Tokyo, Japan	−40
London, England	14
Sydney, Australia	−14
Johannesburg, South Africa	430

nucleon attenuation length at sea level by about 7%. This correction becomes less significant with altitude [32, 35]. The details of the correction are too complex for this review.

A further detailed experiment on the geomagnetic rigidity effect was done by placing a very large (11-ton) detector on a truck and rolling it to all of the locations with stationary cosmic ray detectors in North America; see **Figure 13**. This allowed all of the large detectors to be cross-checked and anomalous distortions removed from their data. An effort was made in this experiment to obtain a wide range of nucleon flux values exactly at sea level. The data show very little scatter about the average curve.

The data of experiments like those shown in Figures 11–13 have been analyzed by many theorists to draw out subtle changes. One study which has a direct bearing on our interests is shown in **Figure 14** [39]. This plot indicates how the sea-level flux of neutrons varies as a function of the geomagnetic rigidity of any location and as a function of the solar cycle (to be discussed later). Going from the geomagnetic equator (GV = 15) to the pole (GV = 0) gives a 2× change in the neutron flux. The solar cycle may add about a 30% change.

Relative neutron flux at major cities

The terrestrial flux of nucleons any place on earth can be estimated by knowing three quantities: the geographic longitude and latitude, and the altitude. The geomagnetic coordinates can be calculated from the geographic coordinates; then, Figure 14 will give the relative nucleon flux for this location at sea level. This sea-level flux is then increased using the nucleon attenuation length from Figure 11 for the altitude and rigidity of that location. Typical examples for cities are given in **Table 6** (New York City is used as a baseline).

Attenuation by concrete shielding

Besides altitude, concrete shielding also greatly affects the flux of hadrons. Portland cement concrete nominally is a 1:2 mix of cement and sand which contains 10% water by weight. This approximates concrete floors and roofs in the United States. Concrete densities may vary by up to 30%, especially if aggregate is included, so any concrete absorption calculation will be a rough estimate unless the details of the material are known.

The only experimental measurement of concrete shielding of cosmic ray nucleons showed an attenuation length of 170 g/cm^2, but this experiment only measured the low-energy neutron component (E_n = 0.001–10 MeV) [18]. We have conducted extensive studies of the absorption of cosmic ray nucleons (energy > 50 MeV) under various types of concrete. The results were quite reproducible, and varied <2% depending on concrete composition. The mean attenuation length for neutrons was measured to be 216 g/cm^2.

Figure 15 shows the attenuation of nucleons above 100 MeV as a function of concrete with a typical density of 2.45 g/cm^3. Ceilings with a foot of concrete lower the cosmic ray intensity by 1.4×.

A theoretical analysis of the attenuation of cosmic ray neutrons in earth has shown that the flux of very low-

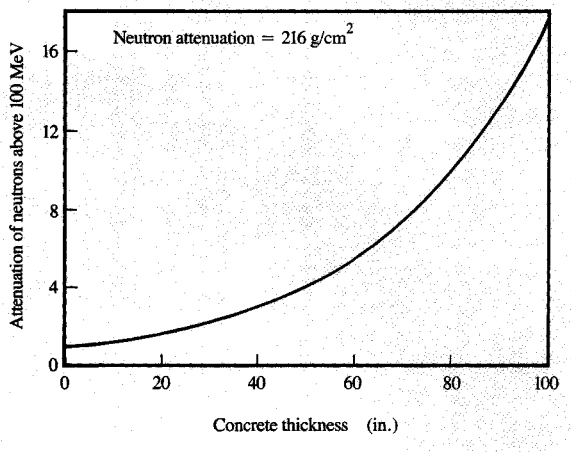

Figure 15

Absorption of cosmic rays by concrete. The attenuation of nucleons by concrete is shown for various thicknesses. Concrete is a material with densities varying from 110–160 lb/ft^3 (1.76–2.56 g/cm^3), so the above curve is a rough approximation. We assume a Portland cement concrete with a 1:2 mix of cement and sand which contains 10% water by weight (no aggregate). This approximates concrete structural floors and roofs in the United States with a density of 152 lb/ft^2 = 2.45 g/cm^2. The absorption of nucleons can be roughly estimated by assuming an exponential attenuation of $1.4x$, where x is the thickness of concrete in feet.

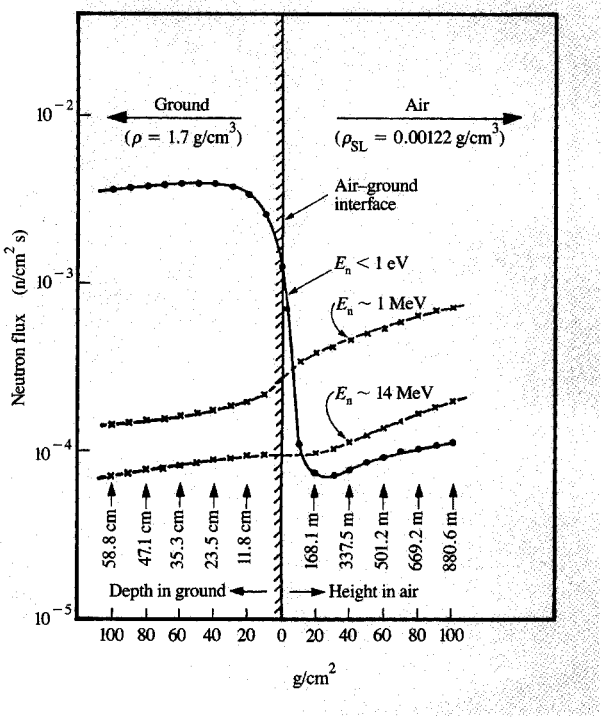

Figure 16

Effects of air–ground interface on neutron spectrum. When the cosmic ray nucleon flux penetrates a solid such as a building, the spectrum of particles suddenly changes. The cascade interactions change from nitrogen and oxygen collisions to collisions with the atoms of the solid. Shown in the figure are the changes of the neutron flux as it penetrates ground (density = 1.7 g/cm^2). The very low-energy neutron flux increases by over 20× within a few centimeters. The higher-energy neutron flux changes less, with neutrons above 100 MeV having no significant change of flux for most typical solids.

energy neutrons may jump 20× after a cm of penetration because of special nuclear reactions which do not occur in atmospheric collisions (**Figure 16**) [40]. This sudden 20× increase in the low-energy neutron flux under earth shielding has been seen in experiments [17]. This increase in the very low-energy neutron flux would lead to an anomalously high attenuation length such as that reported above, but should have little effect on circuit SER because it only changes the flux of low-energy nucleons.

Nucleon flux changes with time

Hundreds of studies have measured the sea-level nucleon flux changes with time. The diurnal effect is less than 10%, again indicating that the sun is not an important source of the sea-level cosmic ray nucleons [5]. The effect of the position of the earth in its orbit is also less than 10% (annual effect).

The eleven-year solar cycle creates an additional magnetic field about the earth, and this field increases the shielding against intra-galactic cosmic rays and sea-level cosmic rays during the period of the active sun. This reduction is about 30% (peak to peak), and about 20% when averaged over the three-year period of the active or quiet sun. The period from 1984 to 1986 was the cycle of the quiet sun, and hence a maximum of sea-level cosmic rays [the peak of sea-level cosmic rays lags slightly out of phase with the solar cycle, and the peak of the sea-level cosmic rays occurred about 1987 (see Figure 1)].

Associated with the solar cycle are solar flares, which add considerable noise (variation) to the 30% total nucleon increase (**Figure 17**). A solar flare so large that it affects the earth's sea-level flux of particles occurs a few times during each active sun. The particles are spread out in time, both because the flare may last a few hours, and also because of the time for particles of different energy to travel from the sun to the earth (a 100-MeV proton takes over two hours to reach the earth). The active sun of 1991–1993 was the most violent ever recorded, with more than a dozen major cosmic ray bursts, similar to that shown, recorded at terrestrial altitudes.

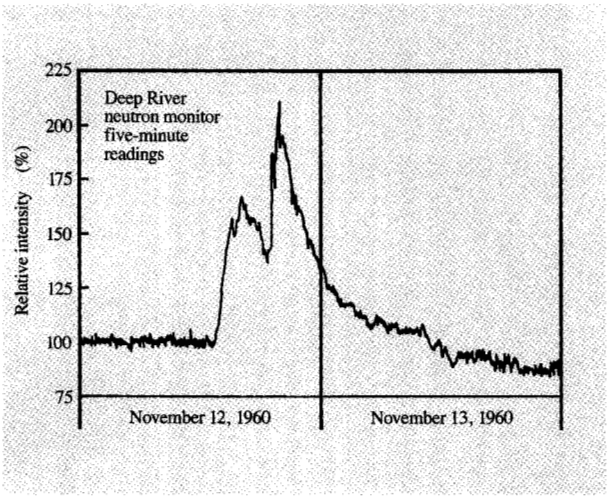

Figure 17

Effects of solar flares on cosmic rays. Large solar flares occur frequently during the active sun period. They emit tight streams of particles which flow out through the solar system. Several times a year the earth may move through such a stream of particles. The curve shows the result at sea level of such a solar flare. There is about a 2× change in energetic sea-level nucleons which lasts for half a day. During the period of quiet sun this type of event never occurs.

Figure 17 shows the signal from a total nucleon flux detector in Canada. This plot is from a flare which occurred in 1960, a year before the active sun of 1961. The flare caused a major pulse in the nucleon flux of approximately 2×. These results are for the largest flares in the 1960 active sun period.

Absolute neutron flux

There have been no quantitative measurements of the total sea-level cosmic ray nucleon flux. There have been separate measurements of the neutron flux (which at sea level is about 90% of the nucleons above 100 MeV) and of the very high-energy proton flux.

Figure 18 shows a collection of experimental cosmic ray measurements, and our evaluation of a nominal neutron flux to be used for sea-level sites in the United States. The solid line is a best guess for a nominal sea-level flux of neutrons. Although the data appear to hug the line closely, there is a possibility of a shift by 2× because of a lack of knowledge of the angular distribution of the neutron flux at sea level.

The problem of assuming an angular dependence of the neutron flux spectrum enters into the neutron flux experiments in two ways (the angular dependence of the flux is defined as the way in which the flux intensity varies with the angle to a horizontal plane). First, any energetic neutron detector has a detection efficiency which changes depending on the direction of the incident neutron. Second, since none of the experiments measured completely how the measured flux changed with angle, the measurements must be modeled to estimate the full hemispherical flux.

All of the papers modeled their results by assuming a cosine variation of flux with angle. To summarize the experimental angular distribution of cosmic ray nucleons at sea level, Reference [41] shows $\cos^3$ for E_n = 200 MeV; Reference [42] shows $\cos^1$ to $\cos^4$ for E_n > 350 MeV; Reference [43] shows $\cos^3$ to $\cos^5$ for E_n = 100–1000 MeV; Reference [29] shows $\cos^{3.5}$ for E_n = 200 MeV; Reference [44] shows $\cos^{2.1}$ to $\cos^{2.6}$ for E_n from 60 to 750 MeV; and Reference [45] shows a $\cos^3$ variation for E_n from 10 to 100 MeV.

A reasonable average of the above is an angular variation of $\cos^3$ for sea-level nucleons from 20 to 1000 MeV.

The correction to a measured vertical neutron flux [in units of flux per steradian (sr)] to obtain a total flux can be made as follows: If the flux is presumed to be isotropic, the total flux is just 2π times the flux/sr in a vertical direction (energetic neutrons come only from above, not

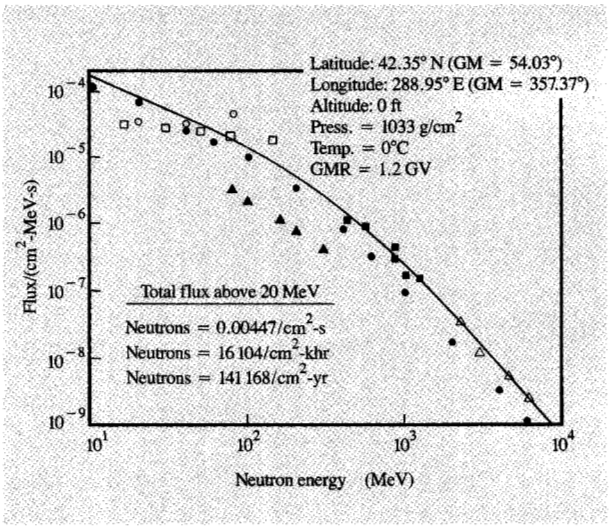

Figure 18

Experimental data on sea-level neutron spectrum. The absolute flux of neutrons above 10 MeV has been measured by six groups. These are shown on the plot and are discussed in detail in the text. All have been normalized to New York City, 1985, as a baseline. The solid curve is the nominal sea-level neutron flux which best fits the data. Although the data were quoted as specific for neutrons, some of the experiments did not remove the contribution of other hadron particles. The curve is suggested as the total nucleon flux curve.

from below). If one assumes a cosine distribution, the multiplicative factor is just π. The general solution for a flux with an angular distribution of $\cos^x$ is the total flux = $2\pi/(x + 1)$ times the angular flux. Using the above experimental average of $\cos^3$ for the neutron angular flux, the total flux is 1.6 times the vertical flux/sr. This is called the "solid angle correction" below.

Another problem with the experimental neutron flux papers is that there is always a correction applied for geomagnetic latitude to obtain a normalized value at 44 N (the reference latitude for sea-level measurements). Few authors discuss how they make this correction.

The data points in Figure 18 are discussed below. Data which have been corrected are noted.

- Reference [22] contains the most comprehensive experimental values of sea-level neutrons. Detectors were flown over northern latitudes at a series of altitudes. This work is so influential that its results may have contaminated later works, which always refer to Hess as the benchmark values. The high-energy values of Hess contained a mistake which was later corrected by Hughes and Martin [23]. These authors pointed out that the Hess detector would convert some of the other cascade particles into neutrons, erroneously increasing the measured neutron flux. This problem they called the "multiplicity" effect, and these criticisms were later verified by many other studies. We show in Figure 18 the Hess values up to 100 MeV, and above this are shown the corrected values [23] removing the counting of detector-generated neutrons. Since the Hess values were determined from an omnidirectional neutron detector, no correction was made for solid angle.
- ■ This paper is by Ashton et al. [46]. Their analysis of the problems of measuring neutron fluxes makes this paper one of the most important in the field. Measurements of other cosmic ray particle fluxes by this group are considered benchmarks. Note: The data values in Figure 18 have been corrected for solid angle.
- ▲ Reference [29] comes from a Ph.D. thesis. For the sea-level spectrum the author detected only 29 high-energy neutrons, and the data may not be reliable.
- ○ Reference [45]. The sea-level data might be presumed to be an afterthought in this paper. The authors used a balloon flight to probe the neutron flux at high altitudes. Before the flight they let the detector sit in a barn at the launch site in Missouri for two weeks and collected 12 hours of data. The flux shown is the result of the pre-launch data, and is of marginal quality.
- △ Reference [47]. This paper from Wolfendale's group at the University of Dundee is for the cosmic ray proton flux at sea level, which should be about equal to the neutron flux for energies above 1 GeV (see Figure 4). The data have been corrected for solid angle.

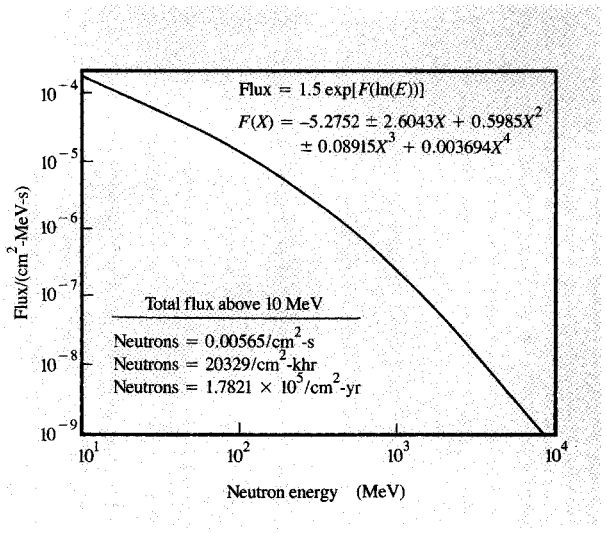

Figure 19

Analytic approximation to neutron flux at New York City. The nominal nucleon flux at sea level (New York City) is shown with an analytic formula which fits the curve to 1%. This formula is not valid beyond the limits of the plot shown.

- □ Reference [48]. This Ph.D. paper is a rigorous examination of the neutron flux at various terrestrial sites based on neutron time-of-flight measurements. Unfortunately, it disagrees with all other data.

Figure 19 shows the nominal neutron flux with a simple analytic formula for the flux (the formula is valid only over the range of neutron energies shown).

- *Pion flux at sea level*

As described at the start of this paper, the various pions are unstable particles with a mass of about 135 MeV and a lifetime of about 26 ns. They have the strong interaction, so they act just like the nucleons except that they have smaller mass. Since there are 100 times as many nucleons as pions at sea level, we expect their SER contribution from the strong interaction to be insignificant.

There is one mode of interaction of pions with matter which makes a unique contribution to a circuit SER. Negative pions have an interaction, pion capture, not found in any other particle in the cosmic shower. It begins when a pion loses all of its kinetic energy within a solid. It then attaches itself to the nearest nucleus and begins to orbit like an electron. But the pion is not an electron, so the Pauli exclusion principle does not keep it outside the electrons. It quickly cascades into tighter orbits, emitting X-rays, until it is in a 1-s orbit. The pion is 200 times the mass of the electron, so its fundamental orbit is smaller

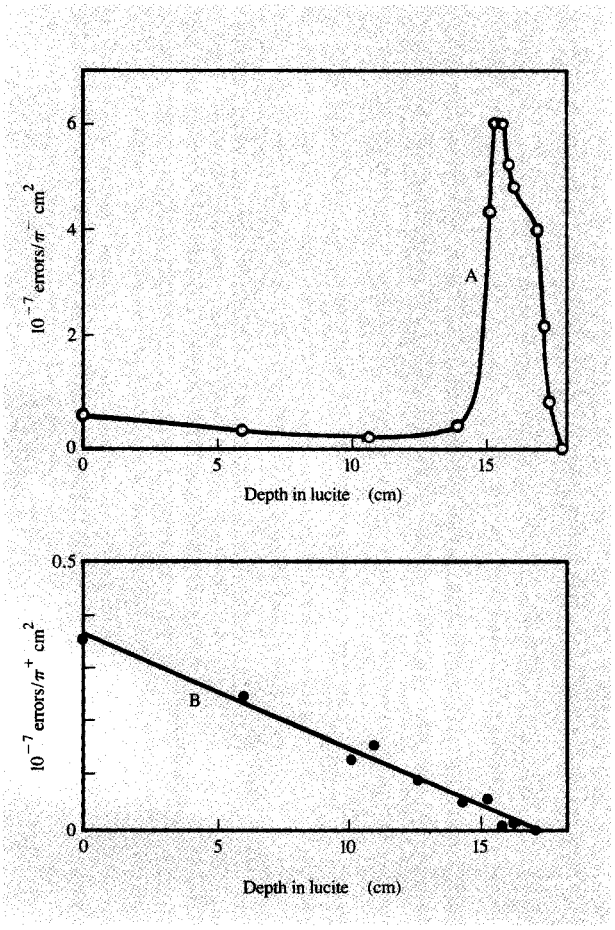

Figure 20

Effect of pion capture on LSI circuits. Experimental SER results from pion irradiation of a 4Kb n-MOS static RAM [48]. Curve A shows the SER cross section per chip as a function of negative pion energy. In the experiment the pion beam energy was lowered by interposing lucite blocks in front of the circuit. The pion energy at the left is 164 MeV, and it decreases to zero at the right. The SER observed for high energy is about the same as that obtained from proton bombardment. At about zero pion energy, the SER rate suddenly jumps 1500%. This low-energy SER is due to pion-capture events (described in the text). To confirm the above result, the same experiment was run with a positive pion beam (Curve B). Positive pions do not undergo pion capture. For high-energy pions, the SER was the same as for the negative pions (note expanded ordinate scale). For low-energy pions, the SER cross section goes to zero. This confirms that the above zero-energy SER result was from pion-capture events.

than the size of the nucleus. Since the pion has the strong interaction, it quickly couples with one of the nucleons, and all of its 135 MeV of mass is transformed into nucleonic energy. The nucleus immediately fissions into many high-energy fragments.

The effect of pion capture on circuit SER has been experimentally tested. **Figure 20** shows an elegant experiment with 164-MeV negative pions [49]. The target of these pions was a 4Kb n-MOS SRAM (AMD-9114) with an SER cross section for nucleon bombardment of about 19×10^{-12} cm^2, which is a typical value for that type of chip. When it was irradiated with energetic pions, the circuit had the same SER cross section that it had under nucleon bombardment, which was to be expected. Then blocks of plastic were introduced in front of the target, reducing the energy of the pion beam reaching the target. After 15 cm of plastic was introduced, the SER cross section suddenly increased by 1500%. This thickness of plastic was almost enough to stop the pion beam, and some of the pions were leaking through the back side and drifting into the circuit. There they underwent the pion capture interaction. It is estimated that *every* negative pion which was captured in the active volume of the target led to a soft fail.

To demonstrate that the SER effect was due to pion capture, the authors left the circuit in place and switched to a positive pion beam. The results are also shown in Figure 20, which shows no SER peak for zero-energy positive pions. The positive pion is repelled by the positive nucleus, and it ends its 26-ns lifetime drifting in the electron sea between atoms. Here it cannot couple its mass energy into nucleons, and this energy is dissipated in ways which do not involve an exploding nucleus.

How important to circuit SER is the pion capture effect? At sea level the number of pions which come to a stop in silicon and undergo pion capture is about 8.5/cm^3-yr [33]. Thus, even if every pion capture leads to a soft fail, there will be only about 0.05 fails per year for a 64KB cache memory. For Denver, the number of stopped pions is estimated to be 48/cm^3-yr in silicon.

- *Muon flux at sea level*

The muon effect is different from the pion effect above. There are 1000 times more muons than pions, but muons do not have the strong interaction to couple energy into nucleons. This coupling is necessary to generate intense local charge bursts which can upset circuits.

Two muon effects which affect circuits are the electrostatic scattering of muons from nuclei (which can induce a nuclear recoil of a target atom), and muon capture, which is similar to the pion capture discussed above.

Calculation of muon electrostatic scattering has been discussed in detail [15, 50]. These models take the sea-level flux of muons and calculate the probability of scattering to induce silicon nuclear recoils. The importance of this effect can be roughly evaluated by considering an electronic device which will upset if it receives >100 fC of local charge. (This is the upset charge, Q_{crit}, below which alpha particles may begin to dominate circuit SER.)

The rate at which muons produce recoiling nuclei which can induce >100 fC is 7/cm^3-yr [33]. This is about the

same as the pion capture rate (discussed above), and is insignificant compared to the nucleon effect on circuit SER.

The second muon effect which might contribute to circuit SER is muon capture. This effect begins the same as for pion capture, discussed above. A muon comes to rest within the silicon lattice. If it is a negative muon, it begins to orbit a positive silicon nucleus. It cascades down through various orbits until it reaches a 1-s orbit, which is within the nucleus itself, since the muon is 200 times the mass of an electron.

At this point, muon capture differs from pion capture. The muon does not have the strong interaction, so it cannot couple directly to the nucleons in the nucleus. Instead, muon capture involves the combining of a negative muon with a proton yielding a neutron and a neutrino. The neutrino carries away most of the muon mass-energy of 106 MeV, leaving the neutron with about 6 MeV. This neutron can interact with the nucleus, causing many possible secondary reactions which have been analyzed in detail [16].

The rate at which muon capture occurs at sea level has been studied by many authors, because this effect is important in generating unusual isotopes which can be used in the geological dating of rocks. The accepted sea-level rate for muon capture, relatively independent of stopping material, is

$$\text{Muon capture rate} = 510/\text{cm}^3\text{-yr}. \tag{14}$$

But in contrast to pion capture, few muon-capture events cause a burst of charge capable of upsetting an electronic device. Most emit no charged particles, and less than 3% emit even an alpha-particle [45, 51]. The maximum alpha-particle emission is

$$\begin{aligned}\text{Muon-induced alpha-particle} &= 15/\text{cm}^3\text{-yr};\\ \text{Muon-induced heavy fragment} &< 1/\text{cm}^3\text{-yr}.\end{aligned} \tag{15}$$

At Denver, these events would increase by only 30%, since the muon flux does not change much with altitude.

Theoretical cosmic ray cascades

This section describes how the terrestrial flux of cosmic rays may be calculated theoretically, based on the original work of O'Brien [17, 52]. The calculation predicts charged particle fluxes (muons, pions, and protons) quite accurately, but it appears to underestimate the neutron flux by about 5×. This is discussed in detail under the previous section on neutrons. This model has been shown to be accurate to better than 2× for relative measurements such as the relative cosmic ray intensity at various cities.

The model uses the approach of the Boltzmann transport equation. The incident flux of particles penetrate the atmosphere, governed by cross sections (functions) which modify the flux by evaluating a) energy loss probability, b) creation of new particles, and c) decrease of flux by absorption of particles. Each of these cross sections depends on the particle type, energy, and lifetime (for unstable particles like pions or muons). The transport equation is set up to show the particle flux spectrum as a function of atmospheric depth. The major assumptions are that the atmosphere is considered a planar slab of varying density, that the cross sections do not depend on the air density, and that the air may be considered to be made of a single nuclear species with an atomic weight of 14.48 amu, an atomic number of 7.22, and an ionization potential of 92.8 eV. All electronic energy loss is assumed to be the relativistic Bethe–Bloch type, i.e., approximately proportional to $\ln(E)/E$.

The following creation/absorption operators are considered:

$$\begin{aligned}&p + \text{air} \Rightarrow \nu_p p + \nu_n n + \nu_\pi \pm \pi \pm + \nu_\pi^0 \pi^0,\\ &n + \text{air} \Rightarrow \nu_p p + \nu_n n + \nu_\pi \pm \pi \pm + \nu_\pi^0 \pi^0,\\ &\pi \Rightarrow \mu + \nu,\\ &\pi^0 \Rightarrow 2\gamma \Rightarrow \text{electromagnetic showers},\\ &\mu \Rightarrow e + 2\nu \Rightarrow \text{electromagnetic showers},\end{aligned} \tag{16}$$

where p = protons, n = neutrons, ν = neutrinos, π = pions, and γ = gamma rays. The details of the cross sections are given in [17, 52, 53]. The cascade terminates at 100 MeV (particles are lost from the cascade below this energy), since the simplified transport assumptions are invalid below this energy. Studies have shown that the local terrestrial surroundings (proximity to rock, water, steel, etc.) have a large effect on nucleon density below 100 MeV. At energies below 1 MeV, these local surroundings may change the local nucleon flux by 10×; see Figure 15. The influence of kaon production is considered negligible in this calculation.

The incident flux of nucleons was shown in Figure 2. One set of data is shown; however, many other sets are available, all with similar agreement to the solid curve which is the analytic function used in the program. The incident primary nucleon flux is assumed to be 70% protons and 30% neutrons. The primary flux is truncated to zero for all particles with energies below the geomagnetic rigidity for the terrestrial location chosen. The geomagnetic rigidity is estimated using the 5° grid tables of M. A. Shea (U.S. Department of Defense) based on the 1980 geomagnetic field model [54–56].

The transport calculation is run with ten incident primary angles to cover various trajectories. Calculations of the effects of barometric pressure or ambient temperature are made by using the equivalent changes to the atmospheric air slab.

Figure 4 showed the result of summing over the hemisphere of possible incoming particles, and weighting the sums with their respective solid angles. The upper right corner of the plot shows the basic data of this calculation. The latitude and longitude of New York City are converted to the equivalent geomagnetic values (based on the 1980 magnetic pole of the earth). The altitude of New York City is set at zero feet. The barometric pressure is normal, 1033 g/cm^2 = 29.9 in. Hg. The temperature is set at 0°C. The geomagnetic rigidity for New York City is 1.7 GeV/amu. Not shown is that the solar cycle is assumed to be at a minimum. We show for the nucleon flux below 100 MeV the slope of nucleons obtained in [18, 22], which are atmospheric sea-level values.

The four particles calculated are the fluxes of neutrons, muons, protons, and pions. The total flux of these particles is shown at the lower left of the plot. Comparing the neutron flux of this figure with the values in Figure 18 shows that there is a serious error in the magnitude of the calculated neutron flux. The fluxes of the pions and muons are independent of the neutron flux, and, as discussed above, they are considered to be quite accurate (within ±30%).

Conclusions

The following summarizes the status of our knowledge of cosmic rays at terrestrial altitudes as they affect circuit soft-error rates (SER).

- The change of particle flux from one city to another is known with great accuracy (better than 20%). This allows SER values determined at one location to be scaled to cities elsewhere. It also allows the field testing of circuit sensitivity to cosmic rays to be done at high altitudes (where the cosmic rays and the circuit fail rate can be 10× greater than at sea level), and these results then can be reliably scaled down to sea level.
- The shapes of the various particle flux spectra (flux vs. energy) are known to better than 2×. There are problems with the absolute normalization of the neutron curves to obtain absolute fluxes. Simple expressions are given which show how to use these fluxes to make quick estimates of the cosmic ray fail rates of computer memory chips.
- The relative SER importance of the various particles at sea level (neutrons, protons, pions, muons, electrons, and photons) is understood. Neutrons are the primary problem.
- The variation of cosmic rays with time is well known, e.g., night/day variation, annual changes, solar cycle changes. The most important is the solar cycle, which may vary SER by 30%.
- Concrete shielding above equipment can produce a significant reduction in circuit SER. Also, modest concrete shielding should allow testing for the portion of circuit SER caused by alpha-particles from circuit and package materials.
- Reliable estimates can be made of the probability of a single cosmic ray shower generating two soft errors simultaneously on separate chips in a system. The probability is insignificant.

The following are the major problem areas:

- The absolute sea-level flux of energetic neutrons (E_n > 100 MeV) is known with an accuracy slightly better than 3×.
- The flux of neutrons with intermediate energy (E_n = 20–100 MeV) causes about 20% of the cosmic-ray-induced bipolar circuit SER, but much less for FETs and CMOS. This neutron intensity is very dependent on local surroundings and may vary by 3×. The details of how this flux varies with surroundings have not been well studied. This local source of neutrons will become more important as devices become more sensitive.

References and notes

1. The primary cosmic radiation is reviewed in a) G. S. West, S. J. Wright, and H. C. Euler, "Space and Planetary Environment Criteria Guidelines for Use in Space Vehicle Developments," *NASA-TM-78119*, 1977; b) J. A. Lesniak and W. R. Weber, "The Charge Composition and Energy Spectra of Cosmic-Ray Nuclei," *Astrophys. J.* **223** (1978); and c) D. F. Smart and M. A. Shea, "Galactic Cosmic Radiation and Solar Energetic Particles," *Report No. ADA 167000*, U.S. Air Force Geophysics Laboratory, 1985.
2. G. Gloeckler, "Composition of Energetic Particle Populations in Interplanetary Space," *Rev. Geophys. Space Phys.* **17,** 569 (1979).
3. S. Hayakawa, *Cosmic Ray Physics*, Wiley-Interscience Publishing Co., New York, 1969. This is the most comprehensive textbook on cosmic rays.
4. A. W. Wolfendale, *Cosmic Rays at Sealevel*, The Institute of Physics, London, 1973. A comprehensive study of experimental results with discussions of their limitations.
5. *Handbook of Geophysics and the Space Environment*, A. S. Jursa, Ed., United States Air Force Geophysics Laboratory, U.S.-N.T.I.S., 1985. Best modern review, but mostly concerns satellite-altitude cosmic rays.
6. L. I. Dorman, *Cosmic Rays*, North-Holland Publishing Co., Amsterdam, 1974.
7. J. G. Wilson, *Cosmic Rays*, Wykeham Publications/ Springer-Verlag, London, 1976.
8. *Handbuch der Physik*, Vol. XLVI/1, S. Flugge, Ed., Springer-Verlag, Berlin, 1961.
9. *Handbuch der Physik*, Vol. XLVI/2, S. Flugge, Ed., Springer-Verlag, Berlin, 1967.
10. A. M. Hilas, *Cosmic Rays*, Pergamon Press, Oxford, 1972.
11. P. Singer, *Springer Tracts in Modern Physics*, Vol. 71, 1971.
12. G. Pfotzer, *Z. Physik* **102,** 23 (1936).
13. V. F. Hess, *Phys. Zeitschr.* **14,** 610 (1913).
14. J. Olsen, P. E. Becher, P. B. Fynbo, P. Raaby, and J. Schultz, *IEEE Trans. Nucl. Sci.* **40,** 74 (1993).
15. A. Taber and E. Normand, *IEEE Trans. Nucl. Sci.* **40,** 120 (1993).
16. J. F. Ziegler and W. A. Lanford, *Science* **206,** 776 (1979).

17. K. O'Brien, *Report No. EML-338*, United States Department of Energy, 1978.
18. M. Yamashita, L. D. Stephens, and H. W. Patterson, *J. Geophys. Res.* **71,** 3817 (1966).
19. T. J. O'Gorman, J. M. Ross, A. H. Taber, J. F. Ziegler, H. P. Muhlfeld, C. J. Montrose, H. W. Curtis, and J. L. Walsh, "Field Testing for Cosmic Ray Soft Errors in Semiconductor Memories," *IBM J. Res. Develop.* **40,** 41–50 (1996, this issue).
20. J. F. Ziegler, H. P. Muhlfeld, C. J. Montrose, H. W. Curtis, T. J. O'Gorman, and J. M. Ross, "Accelerated Testing for Cosmic Soft-Error Rate," *IBM J. Res. Develop.* **40,** 51–72 (1996, this issue).
21. J. F. Ziegler, H. W. Curtis, H. P. Muhlfeld, C. J. Montrose, B. Chin, M. Nicewicz, C. A. Russell, W. Y. Wang, L. B. Freeman, P. Hosier, L. E. LaFave, J. L. Walsh, J. M. Orro, G. J. Unger, J. M. Ross, T. J. O'Gorman, B. Messina, T. D. Sullivan, A. J. Sykes, H. Yourke, T. A. Enger, V. Tolat, T. S. Scott, A. H. Taber, R. J. Sussman, W. A. Klein, and C. W. Wahaus, "IBM Experiments in Soft Fails in Computer Electronics (1978–1994)," *IBM J. Res. Develop.* **40,** 3–18 (1996, this issue).
22. W. N. Hess, H. W. Patterson, R. Wallace, and E. L. Chupp, *Phys. Rev.* **116,** 445 (1959).
23. E. B. Hughes and P. L. Martin, *J. Geophys. Rev.* **21,** 1435 (1966).
24. H. W. Patterson, W. N. Hess, B. J. Moyer, and R. W. Wallace, *Publication No. 8208*, University of California, 1959.
25. J. A. Simpson, W. Fonger, and S. B. Treiman, *Phys. Rev.* **90,** 934 (1953).
26. M. V. K. Apparao, R. R. Daniel, G. Joseph, G. S. Gokale, P. J. Lavakare, and R. Sunderrajan, *Can. J. Phys.* **46,** S1030 (1968).
27. E. Tajima, M. Adachi, T. Doke, S. Kubota, and M. Tsukuda, *J. Phys. Rev. Jpn.* **22,** 355 (1967).
28. B. B. Rossi, *High Energy Physics*, Prentice-Hall, Inc., Englewood Cliffs, NJ, 1954, p. 488.
29. E. Heidbreder, K. Pinkau, C. Reppin, and V. Schonfelder, *J. Geophys. Rev.* **76,** 2905 (1971).
30. J. A. Simpson, *Phys. Rev.* **83,** 1175 (1951).
31. J. A. Simpson and W. C. Fagot, *Phys. Rev.* **90,** 1068 (1953).
32. D. C. Rose, K. B. Fenton, J. Katzman, and J. A. Simpson, *Can. J. Phys.* **34,** 968 (1956).
33. F. Bachelet, P. Balata, E. Dyring, and N. Iucci, *Nuovo Cim.* **35,** 23 (1965).
34. J. C. Barton and M. Slade, *Proceedings of the International Conference on Cosmic Rays*, 1965, p. 1006.
35. See, for example, G. G. Boella, A. Degli, C. Dilworth, G. Giannelli, E. Rocca, L. Scarsi, and D. Shapiro, *Nuovo Cim.* **29,** 103 (1963); D. A. Bryant, T. L. Cline, U. D. Desai, and F. B. McDonald, *J. Geophys. Res.* **141,** 478 (1965); and G. G. Boella, G. D. Antoni, C. Dilworth, M. Panelli, and L. Scarsi, *Earth & Planet Sci. Lett.* **4,** 393 (1968).
36. H. Carmichael, M. Bercovitch, M. A. Shea, M. Magidin, and R. W. Peterson, *Can. J. Phys.* **46,** S10006 (1968).
37. B. C. Raubenheimer and P. H. Stoker, *J. Geophys. Res.* **79,** 5069 (1974).
38. H. Carmichael, M. Bercovitch, J. F. Steljes, and M. Magidin, *Proceedings of the International Conference on Cosmic Rays*, 1968, p. 553.
39. J. Lockwood and W. R. Weber, *J. Geophys. Res.* **72,** 3395 (1967).
40. K. O'Brien, H. A. Sandmeier, G. E. Hansen, and J. E. Campbell, *J. Geophys. Res.* **83,** 114 (1978).
41. N. C. Barford and G. Davis, *Proc. Roy. Soc. Lond.* **214,** 225 (1952).
42. E. Lohrmann, *Nuovo Cim.* **1,** 1126 (1955).
43. S. Miyake, K. Hinotani, J. Katsumata, and T. Kaneco, *J. Phys. Soc. Jpn.* **12,** 845 (1957); *ibid.*, **12,** 113 (1957).
44. M. Conversi and P. Rothwell, *Nuovo Cim.* **12,** 101 (1954).
45. A. M. Preszler, G. M. Simnett, and R. S. White, *J. Geophys. Rev.* **79,** 17 (1974).
46. F. Ashton, H. J. Edwards, and G. N. Kelly, *J. Phys. A: Gen. Phys.* **4,** 352 (1971).
47. G. Brooke and A. W. Wolfendale, *Proc. Phys. Soc.* **83,** 843 (1964).
48. R. Saxena, "Ground Level Atmospheric Neutron Flux Measurements in the 10–170 MeV Range," Ph.D. Thesis, University of New Hampshire, 1990 (available from University Microfilms, Inc.).
49. J. F. Dicello, M. E. Schillaci, C. W. McCabe, J. D. Doss, M. Paciotti, P. Berardo, and J. F. Dicello, *IEEE Trans. Nucl. Sci.* **NS-32,** 4201 (1985).
50. J. F. Ziegler and W. A. Lanford, *J. Appl. Phys.* **52,** 4305 (1981).
51. L. Vilgelmova, V. S. Evseev, L. N. Nikityuk, V. N. Pokovshii, and I. A. Yutlandov, *Sov. J. Nucl. Phys.* **13,** 310 (1971).
52. K. O'Brien, "The Natural Radiation Environment," *Report No. 720805-P1*, United States Department of Energy, 1971, p. 15.
53. F. Hajnal, J. E. McLaughlin, M. S. Weinstein, and K. O'Brien, *Report No. HASL-241*, United States Atomic Energy Commission, 1971.
54. M. A. Shea, D. F. Smart, and K. G. McCracken, *J. Geophys. Res.* **70,** 4117 (1965).
55. M. A. Shea and D. F. Smart, *J. Geophys. Res.* **72,** 2021 (1965).
56. M. A. Shea, D. F. Smart, and J. R. McCall, *Can. J. Phys.* **46,** S1098 (1968).

Received June 16, 1994; accepted for publication January 10, 1995

James F. Ziegler *IBM Research Division, Thomas J. Watson Research Center, P.O. Box 218, Yorktown Heights, New York 10598 (ZIEGLER at YKTVMV, ziegler@watson.ibm.com).*
After receiving B.S., M.S., and Ph.D. degrees from Yale, Dr. Ziegler joined IBM in 1967 at the Thomas J. Watson Research Center, where he now manages the Material Analysis and Radiation Effects group. Most of his research concerns the interaction of radiation with matter. Dr. Ziegler is the author of more than 130 publications and 14 books; he holds 11 U.S. patents. He received IBM Corporate Awards in 1981 and 1990. Dr. Ziegler is a Fellow of the American Physical Society and of the IEEE. He has been awarded the von Humboldt Senior Scientist Prize by the German government.